

PAPER • OPEN ACCESS

Combined current and wind simulation for floating offshore wind turbines

To cite this article: A Otter *et al* 2022 *J. Phys.: Conf. Ser.* **2362** 012028

View the [article online](#) for updates and enhancements.

You may also like

- [The effects of second-order hydrodynamics on a semisubmersible floating offshore wind turbine](#)
I Bayati, J Jonkman, A Robertson et al.
- [A Flexible, Multi-fidelity Levelised Cost of Energy Model for Floating Offshore Wind Turbines Multidisciplinary Design, Analysis and Optimisation Approaches](#)
V Sykes, M Collu and A Coraddu
- [Design and Simulation Analysis of the Transmission Scheme for the Mine Double Speed Winch](#)
Yayun Zhang and Guiyun Xu



ECS
The
Electrochemical
Society
Advancing solid state &
electrochemical science & technology

DISCOVER
how sustainability
intersects with
electrochemistry & solid
state science research

Combined current and wind simulation for floating offshore wind turbines

A Otter^{1,3}, C Desmond², B Flannery¹ and J Murphy¹

¹ Lir National Ocean Test Facility, University College Cork, Haulbowline Road, Ringaskiddy, P43C573, County Cork, Ireland.

² Gavin and Doherty Geosolutions Ltd, Dublin 14, D14 X627, Ireland

³ aldert.otter@ucc.ie

Abstract. This paper describes the validation of a novel method to simulate current loading on a floating offshore wind turbine model. A dynamic winch actuator is used to emulate the drag force of current on the platform of the model with a Software in the Loop application. Current loads are combined with wave- and wind loads. The results of experiments with physical current are validated against the results of experiments with simulated current. A method to simulate wave-current interactions is also described. The results show that the winch actuator can reliably emulate current induced drag forces in comparison with physical current under various combinations of environmental loads. Experimental repeatability of the response of the platform is shown to be superior when using simulated- rather than physical current.

1. Introduction

Combined wave- and wind loads applied to Floating Offshore Wind Turbine (FOWT) scale models in wave basin experiments [1] is well documented in the literature. Environmental loads are either applied with the full physical method, or with the hybrid method during FOWT experiments. With the latter method some of the environmental loads are not applied physically but calculated in real-time and emulated on the model with a mechanical actuator.

Adding current to waves and wind during FOWT experiments in laboratory basins is an additional step towards creating realistic offshore conditions and providing valuable insight for systems design and numerical tool validation. Current loading, although rarely applied during FOWT experimental campaigns, is typically applied using current generation capabilities.

Bachynski et al [2] applied physical current during their tests with a semisubmersible FOWT model but used a hybrid method for wind loads. Gueydon et al [3] compared experiments with the full physical method and the hybrid method for wind loads on a Tension Leg Platform model but also applied physical current for all tests. Utsunomiya et al [4] tested a spar FOWT model under combined wind/wave/current loads with the full physical method.

Bulky and expensive equipment is required to generate physical current in wave basins and this capability is available in only a limited number of facilities at a scale suitable for the testing of FOWT models. Furthermore, it is challenging in a laboratory environment to generate laminar current flows or turbulent flows which are characteristic of real-world flows over more than a limited range dictated by



the facility's operational capabilities and basin lengths. The generation of realistic current flows while also generating realistic waves with low levels of reflection is a further challenge.

In this paper an alternative hybrid method to simulate current loading on a FOWT model is compared to the use of physical current generation. This hybrid method uses a dynamic winch with a Software in the Loop (SIL) application to emulate the resulting drag force from a current on the platform of a FOWT model. The emulation of current induced drag force will be referred to as 'SIL current' in this paper, and physically generated current will simply be referred to as 'physical current'.

The comparison study was conducted in the Wave Current Flume (WCF) at the Lir National Ocean Test Facility (NOTF), Cork, Ireland, with a 1/50 scale model of the INNWIND.EU semisubmersible [5] FOWT. The winch actuator was used in combination with physical waves and a Multi-Propeller Actuator (MPA) for aerodynamic load emulation, which also works with SIL.

2. Current simulation system

A servo motor and a custom-made winch drum make up the winch actuator. The winch cable is connected to the FOWT model on the downstream side via a pulley system on the instrument bridge. A real-time controller, linked with MATLAB/Simulink for the real-time simulation, controls the winch. The drag force is a function of the velocity of the current, and the winch alters the tension in the cable dynamically to emulate the drag force on the platform of the FOWT. Due to motion of the floating platform the relative velocity of the current is constantly changing. By combining the velocity of the current and the velocity of the floating platform the relative velocity is found. The drag force is calculated with the drag term of the Morison equation:

$$F_D = \frac{1}{2} \rho C_D A |U - u| (U - u) \quad (1)$$

Where F_D is the drag force, ρ is the density of water, C_D is a drag coefficient, A is the wetted cross-sectional area of the platform, U is the velocity of the current, and u is the velocity of the platform.

An algorithm in Simulink, based on equation (1), calculates the drag force of the current on the platform for each time step with steady velocity of the current as input. The demanded force/tension is maintained by a Proportion Integration (PI) controller with feedback from a load cell in the winch cable. Real-time velocity data of the platform is provided by a motion tracking system and used to update the relative velocity and drag force of the current for each time step.

The sampling-rate of the motion tracking system and load cell is 32 Hz, the actuation rate of the winch is 25 Hz, and the real-time simulation rate is 22 Hz, giving a time step of 0.045 seconds. For the experiments, a soft mooring system, i.e., horizontal moorings above still water level, is used for station keeping of the model, with three mooring lines in a 120-degree spread. To eliminate non-representative pitch motion of the model from actuation with the winch, the cable is connected to the turbine column of the model at $Z = \text{Centre of Gravity (COG)}$ in a conventional coordinate system. Although the force centre for current on the wetted area of the platform shifts during pitch and heave, any non-representative pitch is expected to be minimal with the cable at COG. Figure 1 shows the model in the WCF in Lir NOTF, and Figure 2 shows the layout of the winch actuator.

3. Wind simulation

The MPA, which is described in [6], emulates rotor thrust and rotor torque of the NREL 5MW turbine at hub height on the model. The original design of the INNWIND semisubmersible FOWT is with the DTU 10MW turbine. However, a comparative study between the MPA and a 1/50 physical scale model of the NREL 5MW turbine is planned for a future date and has dictated the use of the 5MW turbine in this study. Although an unusual combination of platform and turbine, the focus of this study is the simulation method of current in combination with wave- and wind loads. The choice of wind turbine is therefore arbitrary.

Rotor thrust and torque are calculated with another algorithm in Simulink, based on the method described in [7]. A single time-series of turbulent wind around 9 m/s at full scale is used as input for the numerical simulation. A lookup table for the thrust coefficient as a function of Tip Speed Ratio (TSR)

is used for the calculation of rotor thrust. Another lookup table is used to determine rotor torque as a function of rotor speed. These lookup tables were generated with offline simulations of the NREL 5MW turbine in FAST. Thrust- and torque loads are scaled down before emulation with the MPA. All wind loads for any test cases with wind were simulated with the MPA. Wind direction was aligned with wave direction for all test cases.



Figure 1. The FOWT model in the WCF at Lir NOTF, with the MPA at the top of the tower. The tower column is downstream of current direction.

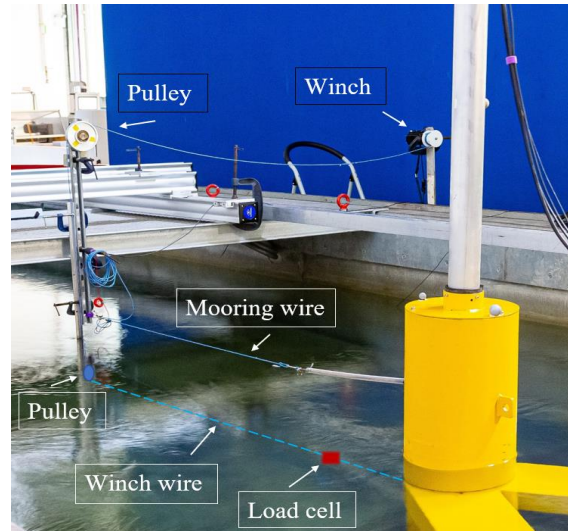


Figure 2. Layout of the winch actuator. The winch is mounted on the basin wall, and the pulley system to the instrument bridge.

4. Physical current and wave-current interactions

Physical current in the WCF is generated by three thrusters mounted in a circulation gallery beneath the floor of the flume. The flow inlet is near the wave maker and the outlet is at the opposite end of the flume near the wave absorbing 'beach'. A smoothing screen with porosity of 44% is mounted vertically in front of the flow outlet and beach. The flow in the WCF can be reversed, however, this renders the smoothing screen ineffective. Therefore, only flow directly opposing the wave direction has been used during experiments.

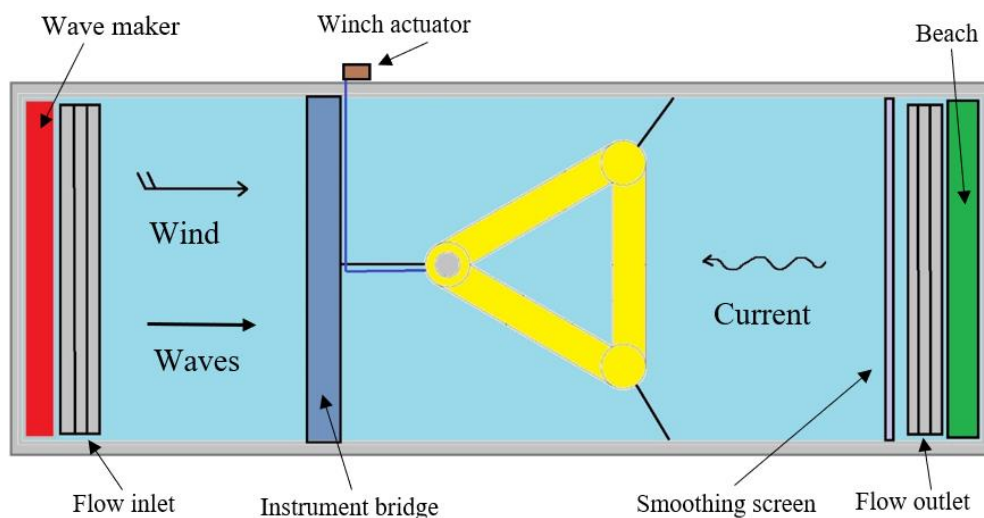


Figure 3. Plan view of the test setup in the WCF. The width/length ratio is exaggerated in this image.

Figure 3 shows a plan view of the model in the WCF, indicating the directions of current, wind, and waves during the experiments. The dimensions of the WCF are somewhat skewed in Figure 3, the actual dimensions of the flume are, Length: 28m, Width: 3m, Depth: 1.2m. The FOWT model is located 17m from the wave maker.

The velocity of the flow was measured on the upstream side of the model at the level of its COG with a Nortek Vectrino acoustic velocimeter, which profiles the water column over a range of 30mm, with a resolution of 1mm. Figure 4 shows the velocity in the X, Y, and Z directions against the percentage of power of the thruster generator, where X is in the longitudinal direction of the flume. The error bars indicate the standard deviation of the measurements. Current velocities used during experiments were 0.11 m/s, 0.14 m/s, and 0.21 m/s, which correspond to 0.75 m/s, 1 m/s, and 1.5 m/s at full scale respectively. The values of C_D in equation (1) were empirically derived for the model over the velocity range shown in Figure 4. The C_D values are shown in Figure 5.

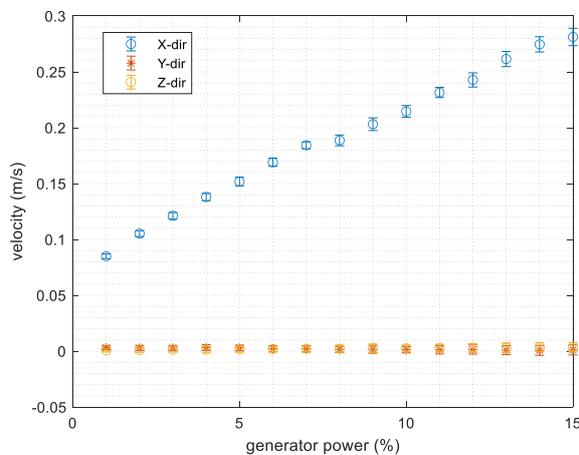


Figure 4. Velocity of the flow in the WCF in X, Y, and Z direction.

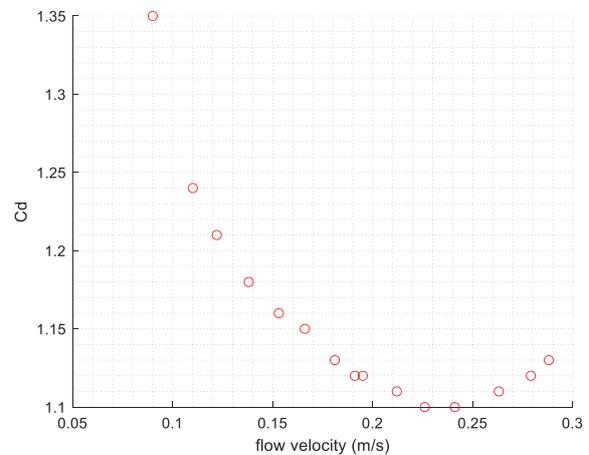


Figure 5. Empirically derived C_D values for the FOWT model.

The well-known phenomena of wave-current interaction is extensively documented in the literature, e.g. Hedges et al [8], and Draycott et al [9]. With an opposing current the spectral energy of an irregular wave time-series will increase. The alteration of wave spectra due to the presence of current is defined by the Huang equation [10]:

$$S_1(\omega) = S(\omega) \frac{4}{\left[1 + \sqrt{1 + (4U\omega/g)}\right]^2 \sqrt{1 + (4U\omega/g)}} \quad (2)$$

Where S_1 is the spectrum with current, S is the spectrum without current, ω is the wave frequency, U is the current velocity, and g is gravitational acceleration.

By altering wave heights and wave steepness, wave-current interaction will influence the response of the platform, particularly in the heave- and pitch Degree of Freedom (DOF). To simulate wave-current interactions with the SIL experiments the wave maker is re-programmed to change the wave heights of an irregular wave spectrum. This results in a wave spectrum with equivalent spectral energy as if a current is present. With physical current only the unaltered, original wave spectrum is used.

Only irregular waves were applied during this study. A wave-only JONSWAP spectrum with $T_p = 1.34$ seconds and $H_s = 0.1$ m at model scale was transformed according to equation (2) for the combined current/wind/wave test cases.

To check the validity of the simulated wave-current interaction, the measured spectra of waves with physical current were compared against measured spectra with SIL current. Initial results showed the

energy of the spectra with SIL current was 15% less on average compared to spectra with physical current. A correction coefficient of 1.13 was added to equation (2) to increase spectral energy. Figure 6 shows the difference with- and without correction of the theoretical spectra. After applying the correction coefficient, the difference in spectral energy between waves with physical current and waves with SIL current was 3% on average. Figure 7 shows the measured spectra with current velocity = 0.21 m/s for physical current and SIL current.

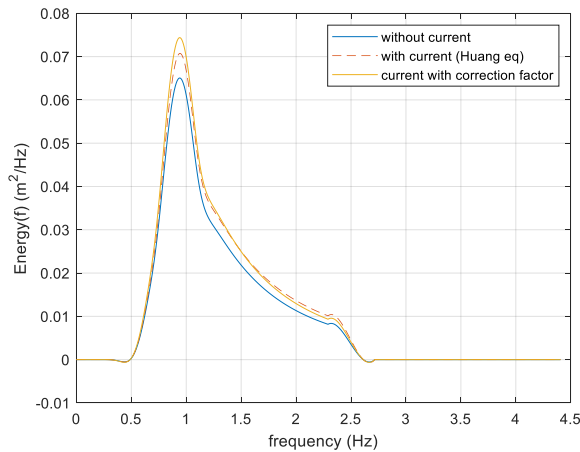


Figure 6. Theoretical wave spectra with- and without current.

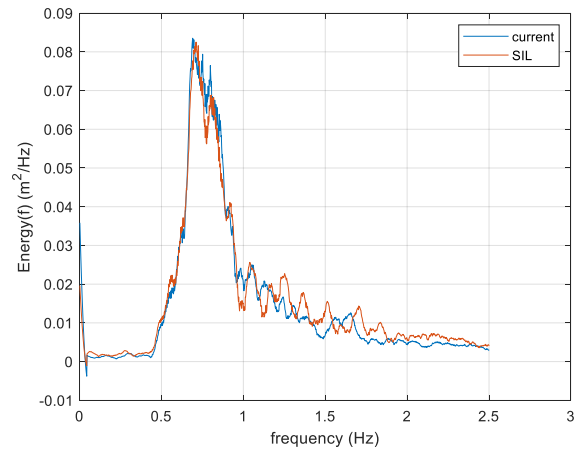


Figure 7. Measured spectra with physical current vs SIL current. Velocity = 0.21 m/s

5. Validation

Three sets of environmental conditions are repeated with physical current and SIL current: current-only, current/wind, and current/wind/waves. The test matrix is shown in Table 1.

For validation the relative difference between experiments with physical current and SIL current is determined for each test case. The relative difference is found by applying the validation metric Relative Error (RE), which is described in [6] and adapted for this study. Each test case is repeated three times and those repeated measurements are combined into an average record. This is done for all the experiments with physical current and SIL current.

Table 1. All Test Cases (TC), which are repeated with physical current and SIL current.

	Current (model scale)	Wind (full scale)	Waves (model scale)
TC 1	0.11 m/s	-	-
TC 2	0.14 m/s	-	-
TC 3	0.21 m/s	-	-
TC 4	0.11 m/s	9 m/s	-
TC 5	0.14 m/s	9 m/s	-
TC 6	0.21 m/s	9 m/s	-
TC 7	0.11 m/s	9 m/s	TP 1.34 s, Hs 0.1 m
TC 8	0.14 m/s	9 m/s	TP 1.34 s, Hs 0.1 m
TC 9	0.21 m/s	9 m/s	TP 1.34 s, Hs 0.1 m

The spectral energy of platform surge, heave, pitch, and mooring tensions of these average records of test cases with physical current are compared against the equivalent test cases with SIL current to determine RE, which is defined as:

$$RE = 1 - \left(\frac{\overline{E_P}}{\overline{E_S}} \right) \quad (3)$$

Where E_P is the spectral energy of the records with physical current, E_S is the spectral energy of the records with SIL current, and the overbar indicates the average records. A perfect match between the physical- and SIL records would give an RE of zero.

As RE is a direct comparison between experimental results, some potential sources of error and uncertainty may affect the metric. For example, repeatability of the experiments will affect the average records and therefore influence RE. A source of uncertainty is the pulley system of the winch actuator. Low-friction pulleys were used; however, any amount of friction may increase the surge damping of the platform during the SIL current experiments. Another source of uncertainty is C_D in equation (1). The accuracy of C_D will have significant influence on the demanded drag force during SIL current experiments. The blockage by the FOWT model across the width of the WCF is also a source of uncertainty. With a maximum breadth of 1.6m, the FOWT model covers just over half the width of the flume and the blockage may influence the response of the model during physical current experiments. However, during SIL current experiments the boundary layers along the basin walls are ignored.

6. Results

For the current-only cases the model is pulled against a fixed barrier upstream of the model. While current is running the model is released and the surge motion of the model is allowed to decay and eventually settle at some distance from the start position.

Figure 8 shows the plotted surge motion of the average records with physical current and SIL current for TC 3. Although the decay oscillations are larger with physical current, the model settles at roughly the same surge distance with physical current and SIL current. Similar patterns were achieved with TC1 and TC 2. The period of the oscillations is slightly longer with SIL current; 1.03 times longer compared to physical current. The smaller oscillations show there is indeed surge damping of the model by the pulley system with SIL current, which also leads to a slightly larger natural period of the surge DOF. Figure 8 also shows there are some small random oscillations after settling with physical current. These are caused by vortex shedding around the columns of the model. Vortex shedding is not simulated with SIL current.

Figure 9 shows the demanded tension and the measured tension in the winch wire for TC 3 with SIL current. While the model is held at the start position the measured tension is around 11 N and demanded tension is 0 N. As the model is not moving, no tension is demanded. However, when the model is released and starts moving, demanded tension follows the same pattern as measured tension. There is a small phase shift between demanded- and measured tension caused by the spring in the winch wire. When RE is applied to compare measured- vs demanded tension an average value of 0.015 is found for the current-only test cases, 0.024 for current/wind cases, and 0.074 for current/wind/wave cases.

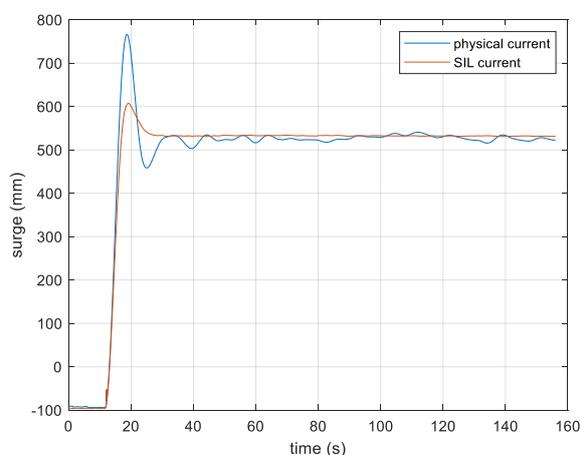


Figure 8. Surge motion of the FOWT model for TC 3 with physical- and SIL current

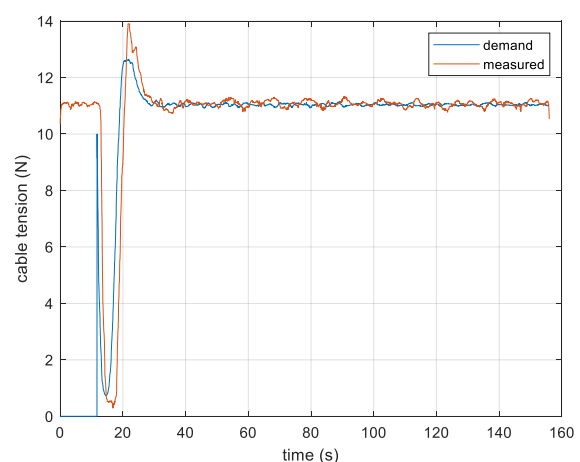


Figure 9. Demanded and measured tension in the winch wire for TC 3 with SIL current.

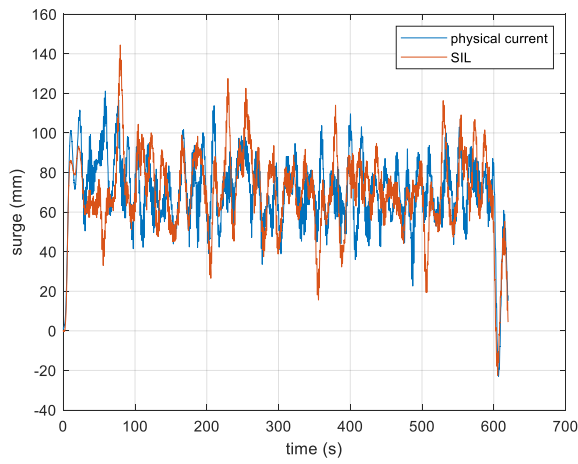


Figure 10. Surge motion for TC 7

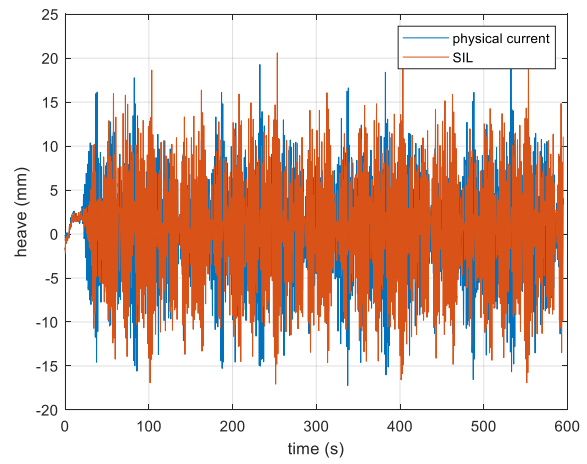


Figure 11. Heave motion for TC 7

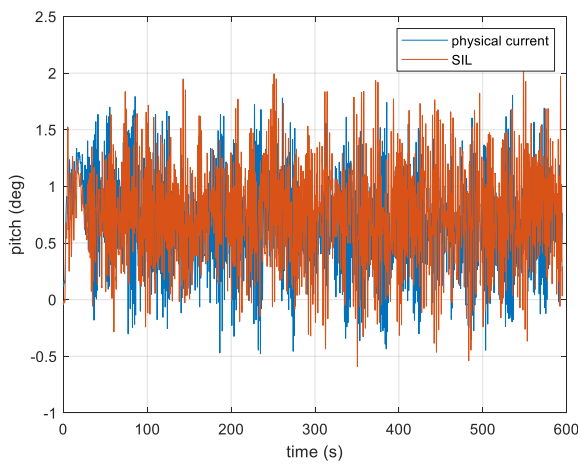


Figure 12. Pitch motion for TC 7

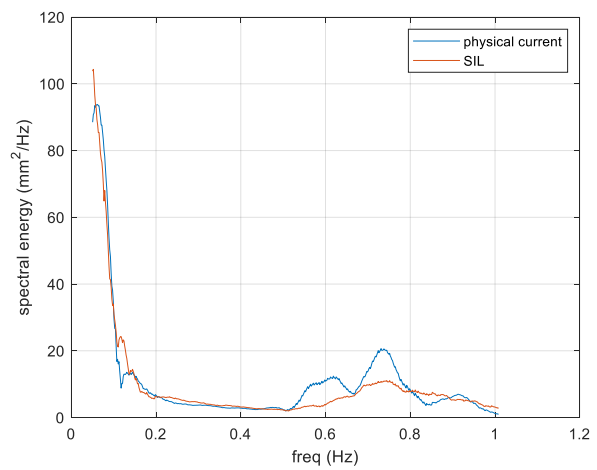


Figure 13. Spectral energy of surge, TC 7

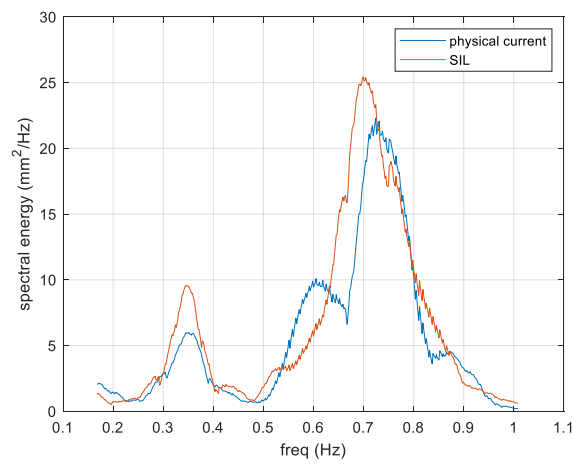


Figure 14. Spectral energy of heave, TC 7

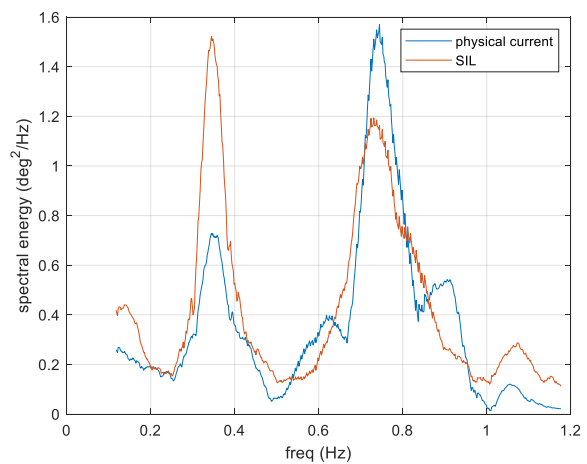


Figure 15. Spectral energy of pitch, TC 7

For TC 4 – 9 current is applied before recording and the start position of the model is the settled surged distance with current. Then, wind and waves are applied according to the test cases. As an example, the results of TC 7 are shown. Figures 10 – 12 show the surge-, heave- and pitch response of the model respectively for TC 7 with physical current and SIL current. Figures 13 – 15 show the spectral energy of the surge-, heave and pitch DOFs of the model for TC 7 with physical current and SIL current. Figure 16 shows the upstream mooring tension for TC 7, and Figure 17 shows the spectral energy of the upstream mooring tension for TC 7. All results shown are at model scale.

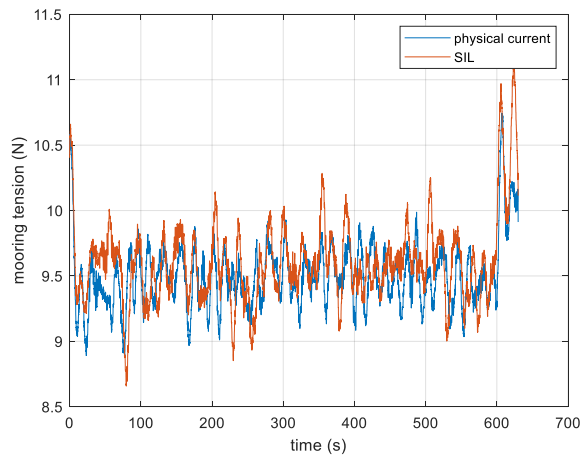


Figure 16. Upstream mooring tension, TC 7

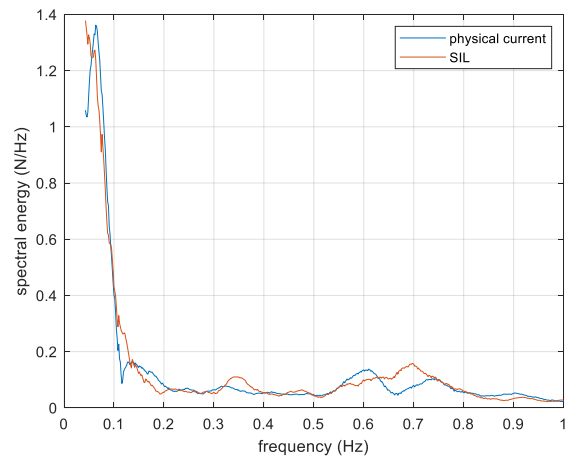


Figure 17. Spectral energy of upstream mooring tension, TC 7

Data from each experiment for TC 4 – 9 between $t = 20$ seconds and $t = 600$ seconds were used for the calculation of RE to make sure current, wind and waves are all acting on the model.

All results for RE of the motion response of the FOWT model and mooring tensions for all test conditions are shown in Table 2. There was no significant pitch- or heave motion during the current-only cases, and no significant heave motion during the current/wind cases. Therefore, only results for surge are given for TC 1 – 3, and results for surge and pitch for TC 4 – 6. Results for surge, heave, and pitch are given for the current/wind/wave cases, TC 7 – 9.

Table 2. RE for surge, heave, and pitch of the platform, and for mooring tensions

	Surge	Pitch	Heave	Mooring tension
TC 1	0.020	-	-	0.017
TC 2	0.023	-	-	0.016
TC 3	0.004	-	-	0.017
TC 4	0.013	0.431	-	0.026
TC 5	0.156	0.142	-	0.068
TC 6	0.087	0.117	-	0.040
TC 7	0.044	0.149	0.189	0.027
TC 8	0.080	0.101	0.162	0.027
TC 9	0.100	0.080	0.072	0.026

7. Discussion

The results clearly show that the response of the model with simulated current compares well to response of the model with physical current for all test conditions, with RE staying below 0.2 for most cases. The exception is pitch motion with wind, and current of 0.11 m/s (TC4). The pitch natural frequency of the

FOWT model is around 0.35 Hz and for all test cases with wind the spectral energy of pitch is higher around this frequency with SIL current compared to physical current, possibly due to the moment created by the connection of the winch cable and the centre of thrust of the MPA during SIL current experiments.

An important reason to simulate current with FOWT experiments is to examine the effect on mooring tensions, which may influence fatigue life and structural integrity of the platform. Good results were achieved for mooring tensions; RE is lower than 0.07 for all test conditions, meaning there is close comparison between physical current and SIL current. Another important reason for current simulation is the alteration of wave shapes due to wave-current interaction and the effect this may have on platform heave and pitch, and hence on accelerations acting on the turbine. Heave- and pitch RE remains below 0.2 for all test cases with waves. This suggests that the method to simulate wave-current interactions with the adjusted wave spectra is adequate.

Good results were achieved for platform surge with SIL current for all test cases, the large blockage ratio of the model in the flume does not affect results, where $RE \leq 0.15$, which suggests that the values of C_D in equation (1) are correct. These validated C_D values can be used for the calibration of numerical models with the INNWIND semisubmersible FOWT.

Table 3. Pearson Correlation Coefficient of surge response for TC 3 and TC 9.

	Experiment 1	Experiment 2	Experiment 3
TC 3 with SIL current	1	1	0.9999
TC 3 with physical current	1	0.9963	0.9940
TC 9 with SIL current	1	0.9848	0.8610
TC 9 with physical current	1	0.8968	0.6487

Repeatability was found to be good with SIL current, although it reduced when all three environmental loads were combined. Repeatability is less favourable with physical current. As an example, the Pearson correlation coefficient for surge response of the FOWT model for the repeated experiments of TC 3 and TC 9 is given in Table 3, where the first experiment is the reference.

Future work will include fine tuning the PI controller for the winch tension. The current-only test cases (TC 1 – 3) show there is higher damping and slightly lower stiffness in the surge DOF of the platform with SIL current compared to physical current. Fine tuning the PI controller of the winch may resolve this.

Further future work will include using the SIL method with catenary moorings on the model rather than the soft mooring system used for this study. The soft mooring system was used to keep the SIL current method as robust and simple as possible. It allows for the current to be assumed as uniform and ignores the vertical shear profile of the water column and hydrodynamic loading on the moorings. With catenary moorings fixed to the bottom of the basin, shear profile and hydrodynamic loading can no longer be ignored and will have to be accounted for in the real-time numerical simulation.

Despite some limitations and uncertainties, the results show that SIL current can reliably emulate current loads on the FOWT model in combination with wind and waves. The advantage of this method is that it can be used in any wave basin without the need for bulky and expensive equipment to generate physical current for a range of test conditions. Furthermore, creating a realistic boundary layer with low turbulent flow, while also limiting wave reflection in the basin when applying physical current, is challenging. A disadvantage of SIL current is that not all response to current loading is captured, such as surge and sway motion of the platform due to vortex shedding.

8. Conclusion

A novel hybrid method to emulate current induced drag force is compared with physical current in this paper. The SIL current method uses a dynamic winch actuator to emulate the drag force of a current on a 1/50 scale model of the INNWIND.EU semisubmersible FOWT. The winch actuator is used in combination with a MPA, which emulates aerodynamic loads. The SIL current method is validated by comparing experimental results with SIL current against experimental results with physical current.

Wave-current interactions are simulated by transforming a JONSWAP spectrum according to the Huang equation and including a correction coefficient. This gives a wave spectrum with equivalent energy as if a physical current is present in the wave basin. A validation metric, RE, is applied to the results for comparison between SIL current and physical current. A perfect match between the two methods will result in $RE = 0$. Results show RE remains below 0.2 for all test conditions, except for pitch motion of the model during the current/wind test case with current velocity of 0.11 m/s. Repeatability of the experiments is better with SIL current compared to experiments with physical current. The real-time numerical simulation does not capture vortex shedding around the columns of the model, which is therefore not simulated during experiments with SIL current. Regardless, the SIL current method can reliably simulate most effects of current loads on the FOWT model in combination with wind and wave loads.

Acknowledgements

The authors would like to acknowledge Christian van den Bosch for his assistance with the instrumentation in Lir NOTF, and the customer service of Schneider Electric for their technical assistance with the servo motor.

This work was funded by Science Foundation Ireland under the PhD fellowship programme.

References

- [1] A. Otter, J. Murphy, V. Pakrashi, A. Robertson, and C. Desmond, "A review of modelling techniques for floating offshore wind turbines," *Wind Energy*, 2021, doi: 10.1002/we.2701.
- [2] E. E. Bachynski, T. Sauder, M. Thys, V. Chabaud, and L. O. Sæther, "Real-time hybrid model testing of a braceless semisubmersible wind turbine. Part 2: experimental results," in *Proceedings of the ASME 2016 35th International Conference on Ocean, Offshore and Arctic Engineering OMAE2016 June*, 2016, no. OMAE2016-54437, pp. 1–12.
- [3] S. Gueydon, R. Lindeboom, W. van Kampen, and E.-J. de Ridder, "COMPARISON OF TWO WIND TURBINE LOADING EMULATION TECHNIQUES BASED ON TESTS OF A TLP-FOWT IN COMBINED WIND, WAVES AND CURRENT," in *Proceedings of the ASME 2018 1st International Offshore Wind Technical Conference IOWTC2018*, 2018, pp. 1–11.
- [4] T. Utsunomiya, S. Yoshida, H. Ookubo, I. Sato, and S. Ishida, "Dynamic analysis of a floating offshore wind turbine under extreme environmental conditions," *J. Offshore Mech. Arct. Eng.*, 2014, doi: 10.1115/1.4025872.
- [5] F. Sandner *et al.*, "INN WIND.EU Deliverable D4.3.3 - Innovative Concepts for Floating Structures," 2015.
- [6] A. Otter, J. Murphy, and C. J. Desmond, "Emulating aerodynamic forces and moments for hybrid testing of floating wind turbine models," in *Journal of Physics: Conference Series*, 2020, doi: 10.1088/1742-6596/1618/3/032022.
- [7] C. Matoug, B. Augier, B. Paillard, G. Maurice, C. Sicot, and S. Barre, "An hybrid approach for the comparison of VAWT and HAWT performances for floating offshore wind turbines," in *Journal of Physics: Conference Series*, 2020, doi: 10.1088/1742-6596/1618/3/032026.
- [8] T. S. Hedges, K. Anastasiou, and D. Gabriel, "Interaction of Random Waves and Currents," *J. Waterw. Port, Coastal, Ocean Eng.*, vol. 111, no. 2, pp. 275–288, Mar. 1985, doi: 10.1061/(ASCE)0733-950X(1985)111:2(275).
- [9] S. Draycott *et al.*, "Re-creation of site-specific multi-directional waves with non-collinear current," *Ocean Eng.*, vol. 152, pp. 391–403, Mar. 2018, doi: 10.1016/J.OCEANENG.2017.10.047.
- [10] N. E. Huang, D. T. Chen, C.-C. Tung, and J. R. Smith, "Interactions between Steady Non-Uniform Currents and Gravity Waves with Applications for Current Measurements," *J. Phys. Oceanogr.*, vol. 2, no. 4, pp. 420–431, 1972, doi: 10.1175/1520-0485(1972)002<0420:ibswuc>2.0.co;2.